Hindawi
Advances in Condensed Matter Physics
Volume 2023, Article ID 9933049, 8 pages
https://doi.org/10.1155/2023/9933049

Research Article

Electronic Properties of a Novel Boron Polymorph: Ogee-Borophene

B. Sarikavak-Lisesivdin and S. B. Lisesivdin

Department of Physics, Faculty of Science, Gazi University, 06500, Teknikokullar, Ankara, Türkiye

Correspondence should be addressed to S. B. Lisesivdin; bora@gazi.edu.tr

Received 3 August 2023; Revised 5 October 2023; Accepted 11 October 2023; Published 27 October 2023

Academic Editor: Sergio Ulloa

In this computational study, a novel borophene polymorph, Ogee-Borophene, characterized by irregular decagon-shaped hollows was reported. The structure involves a deviation from hexagonal configurations found in all other known borophene polymorphs. The decagon-shaped hollow is highly related to the anisotropy of the structure, which results in three types of boron atoms with different electronic properties in the structure. In the study, the electronic structure and density of states of this novel structure were investigated with the help of density functional theory calculations. The electronic structure of Ogee-Borophene shows Dirac cone formations near the Fermi level. The discovery of a novel borophene polymorph, Ogee-Borophene, with irregular-shaped hollows represents a different point of view in the 2D materials field. The unique electronic properties of this material suggest that Ogee-Borophene has the potential to be used in a variety of applications, including transistors, and selective sensor applications without the need for additional doping.

1. Introduction

With the discovery of graphene, especially in the last decade, interest in other 2-dimensional (2D) materials has increased [1, 2]. In the studies that emerged as a result of this interest, it was seen that 2D materials have different and rich properties from each other [3]. When these 2D materials are classified, it is seen that a few species such as silicene, germanene, arsenene, phosphorene, antimonene, stanene, bismuthene, tellurene, and borophene are composed of a single element [4–12].

For the last 20 years, 2D boron nanosheets, 0D nanoclusters, and 1D nanotubes have attracted great interest as research topics [13–25]. Borophene, which is a 2D allotrope of boron, was synthesized in 2015 by Mannix et al. [26] on an Ag(111) substrate under vacuum conditions. The experimental realization of borophene attracted tremendous interest due to its extraordinary electronic and mechanical properties [27]. In terms of electronic structure, while most 2D materials are as investigated as insulators, semimetals, or semiconductors, borophene, and other boron allotropes are found to be metals [28]. Therefore, borophene and other boron allotropes provide a strong base for future nanoelectronic applications as a 2D metal [27]. In terms of mechanical properties, borophene shows an anisotropic structure and structural polymorphism, which also gives tunable electronic properties to borophene and its polymorphs [29]. Normally, it can be predicted that flat boron sheets may form a triangular bonding configuration. However, this configuration is unstable due to excess electrons occupying the antibonding orbitals [30]. The structure of borophene can only be stabilized by the introduction of vacancies. A hollow-hexagon-shaped vacancy-mediated superstructural motif structural polymorphism is suggested and the structural stability and diversity of elemental boron layers are evaluated by treating them as a pseudo alloy $B_{1-x}Va_x$, where Va is a vacancy in the close-packed triangular B lattice [29]. Therefore, many different studies report structures with different hexagonal hollow concentrations and are investigated to find stable free-standing and grown-on structures [31–35].

With the increasing experimental studies, it is found that the substrate is affecting the ground state of the 2D borophenes [32]. The preferred 2D-grown polymorph is found to be a flat $\nu_{1/6}$ type sheet on Ag, Cu, and Ni substrates. But, on an Au substrate, a $\nu_{1/12}$ type buckled sheet is found to be

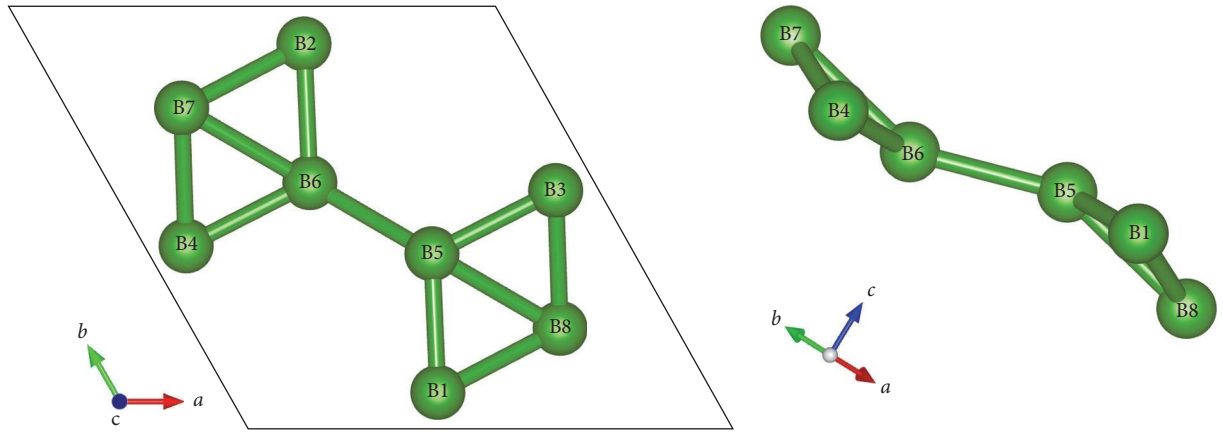

(a) (b)

Figure 1: Atomic structure of Ogee-Borophene from (a) top and side (b) view.

preferred [36]. On experimental Ag(111) growths and its calculations [36], hollow-hexagons chains are found to be aligned as separated by hexagonal boron rows (named β_{12}) or narrower zigzag boron rows separated by hole arrays (named χ_3), which shows the alignments of these vacancies can be changed by different substrates and it is important to study other possible alignments and vacancy types. However, to our knowledge, no study has been reported about the investigation of any other hollow vacancies in borophenes.

In this study, we utilize first-principle density functional theory (DFT) to suggest a new polymorph with irregular decagon-shaped hollows. Because this vacancy is not regular-shaped, which is more like an ellipse than a circle, the irregularity of the vacancy's shape will induce different electronic properties to different atoms in the vicinity of the vacancy. Our study demonstrates the different electronic properties of different boron atoms provide tuning or selective interaction functionality to this newly suggested 2D metallic polymorph with the shape of an Ogee pattern.

2. Computational Details

The structure considered in this work was built and relaxed using the Atomic Simulation Environment (ASE) software package [37]. All the calculations were carried out using DFT where the wave functions are expanded in plane waves as implemented in the grid-based projector-augmented wave (GPAW) code [38, 39]. In calculations, we have used the *gpaw-tools* scripts to interact with ASE and GPAW, create, read, manipulate, and analyze output data and other user interface needs [40]. The crystal structures and electron density maps were visualized using the VESTA software [41]. The exchange–correlation energy is described by the generalized gradient approximation (GGA) using the Perdew–Burke–Ernzerhof (PBE) functional. A vacuum space of 20 Å in the normal orientation of the Ogee-Borophene sheet was used to avoid interactions between the neighboring sheets. The calculations were performed on a C2/m (12) space group cell. The plane-wave cutoff energy was 700 eV. The k-point-mesh for Brillouin zone sampling of primitive cells, based on the Monkhorst–Pack scheme was $9 \times 9 \times 1$. All atoms were allowed to relax until forces were below 0.05 eV Å^{-1}. Phonon dispersion calculation with a $3 \times 3 \times 1$ supercell was performed using Phonopy code [42].

Table 1: Bond lengths in the studied structure.

Bonds (between atoms)	Bond length (Å)
B1–B5, B2–B6	1.63536
B5–B6	1.74326
B4–B6, B3–B5	1.63518
B6–B7, B5–B8	1.78746
B4–B7, B3–B8	1.67638
B1–B8, B2–B7	1.67615
B2–B8, B1–B7	1.65482
B4–B8, B3–B7	1.65459
B1–B2, B3–B4	1.63338

Table 2: Angles of the bonds of the Ogee-Borophene structure.

Atoms path for angle (atom names)	Angle (°)
B2–B6–B5	121.3403
B4–B6–B7	58.4512
B1–B8–B3	110.4173
B5–B1–B7	168.7295

3. Results and Discussion

Figure 1 shows the atomic structure of Ogee-Borophene used in the calculations for a unit cell. The unit cell of Ogee-Borophene consists of eight boron atoms. Figure 1(b) shows the side view of the structure shows an S-shaped buckled behavior. The calculated bond lengths and angles are listed in Tables 1 and 2, respectively. Because of the irregular bond lengths distributed in the structure, the hollow has 10 sides instead of six. Therefore, it is clear that the structure can be suggested to be a polymorph of a Borophene with irregular decagon-shaped hollows.

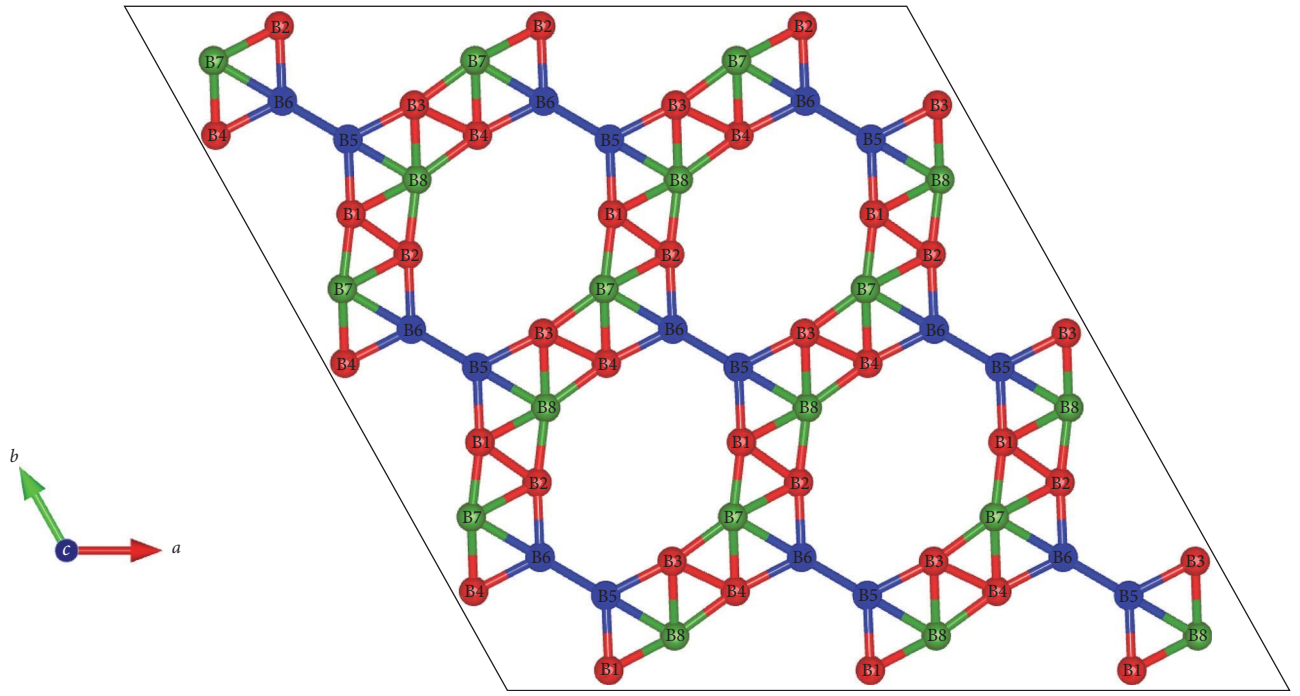

FIGURE 2: 3 × 3 supercell of Ogee-Borophene structure. Boron atoms are colored according to their places with respect to irregular hollow decagons.

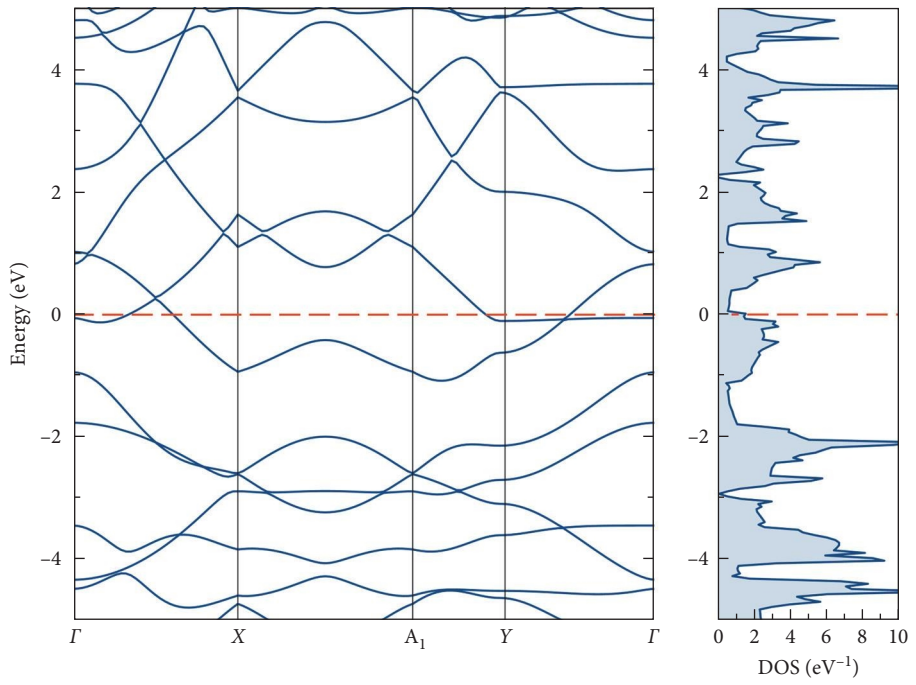

FIGURE 3: Band structure and density of states (DOS) for the Ogee-Borophene.

Figure 2 shows a 3 × 3 supercell of the investigated structure. Different colors of boron atoms represent similar atom types in the structure. The mentioned irregular hollow decagon is shown in Figure 2. For the rest of the article, we will use the α, β, and γ naming for the red, blue, and green represented boron atom types, respectively.

Figure 3 shows the band structure and the density of states (DOS) results of the unstrained Ogee-Borophene structure. Like the other allotropes and polymorphs of borophene, Ogee-Borophene also shows metallic behavior. There are several Dirac cone formations observed in the band structure however, the ones near the Fermi level in

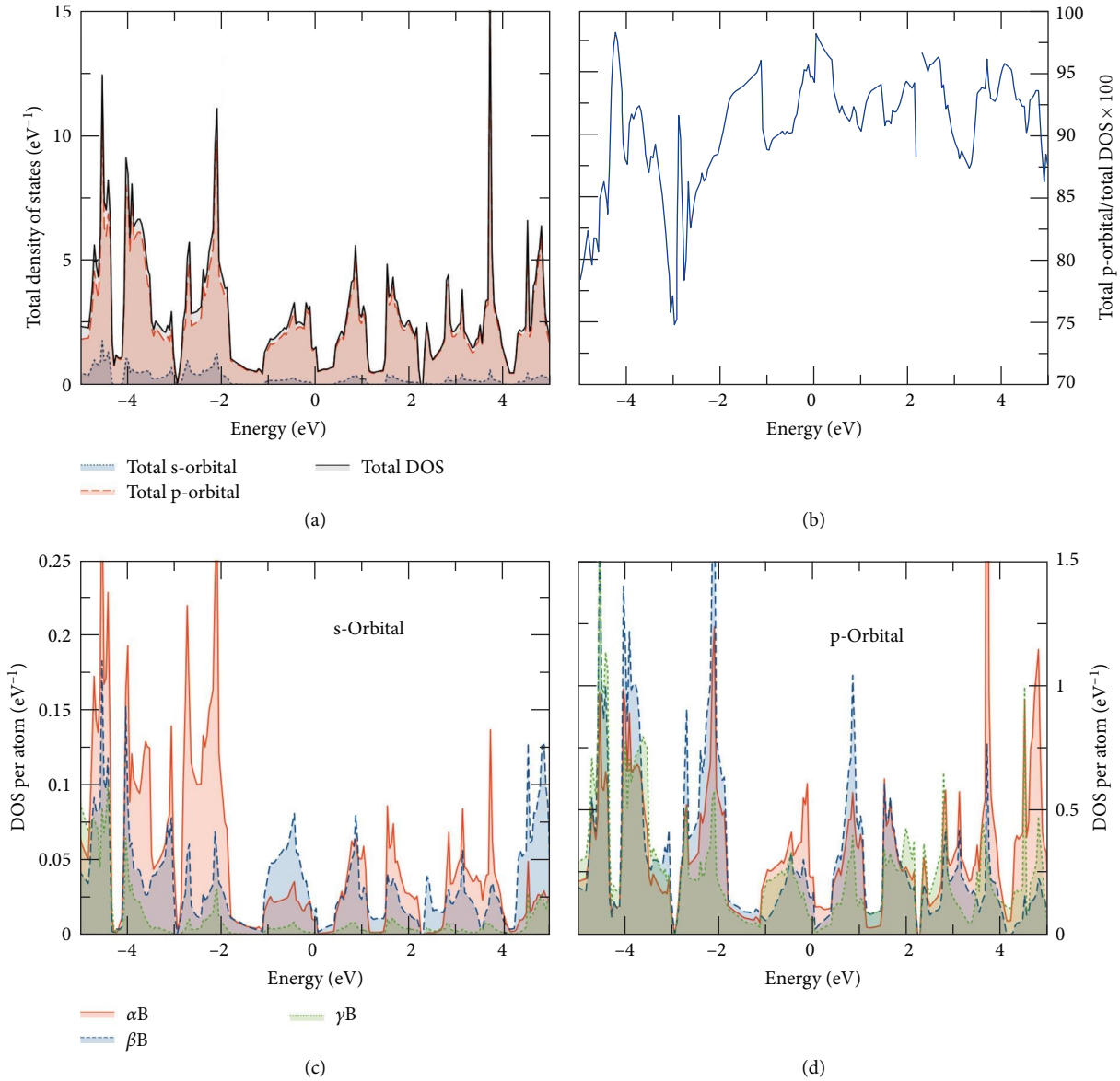

FIGURE 4: PDOS of (a) total-s and (b) total-p orbitals, percentage of p-orbital behavior of state (c) s- and (d) p-orbital contributions for α, β, and γ, types of boron atoms. The Fermi level is located at 0 eV.

between $\Gamma - X$ region and $Y - \Gamma$ region at 0.3 or -0.02 eV can be attributed as interesting, respectively. At this point, state density becomes zero which can be further changed by applying strain or using a substrate. However, these further possible manipulations are out of the scope of this study and can be the subject of another study.

To better understand the electronic structure of the investigated structure, projected DOS (PDOS) behavior is investigated in Figure 4. Figure 4(a) shows that most of the states show p-orbital behavior. In Figure 4(b) the percentage of p-orbital behavior of the states is shown. Near the Fermi level, p-orbital behavior shows a maximum, where we can conclude a possible conductivity of this metal is near a complete p-orbital related. Near the Dirac cone, the graph is not continuous because of zero states at that energy level. To understand better the source of the states near the Fermi level, we investigated the PDOS behaviors of each atom type, which are named α, β, and γ in Figures 4(c) and 4(d). Near the Fermi level, s-orbital states of β-boron and p-orbital states of α-boron are dominated. Because the p-orbital is dominant at the Fermi level, it can be suggested that the p-orbital states of α-boron are deciding the nature of the conduction in the investigated structure.

In Figure 5, PDOS of the p_x, p_y, and p_z orbitals are shown for α, β, and γ types of boron atoms which are mentioned before. Because of the structural anisotropy of the Ogee-Borophene, it is not possible to any similarities between p_x and p_y orbitals. For α and β types, valance electrons are highly p_y orbital dominated. And for β and γ types, conduction electrons are highly p_z orbital dominated. Although the conduction electrons in the α-type boron atom are generally in the p_x orbital characteristic, it is possible to observe that

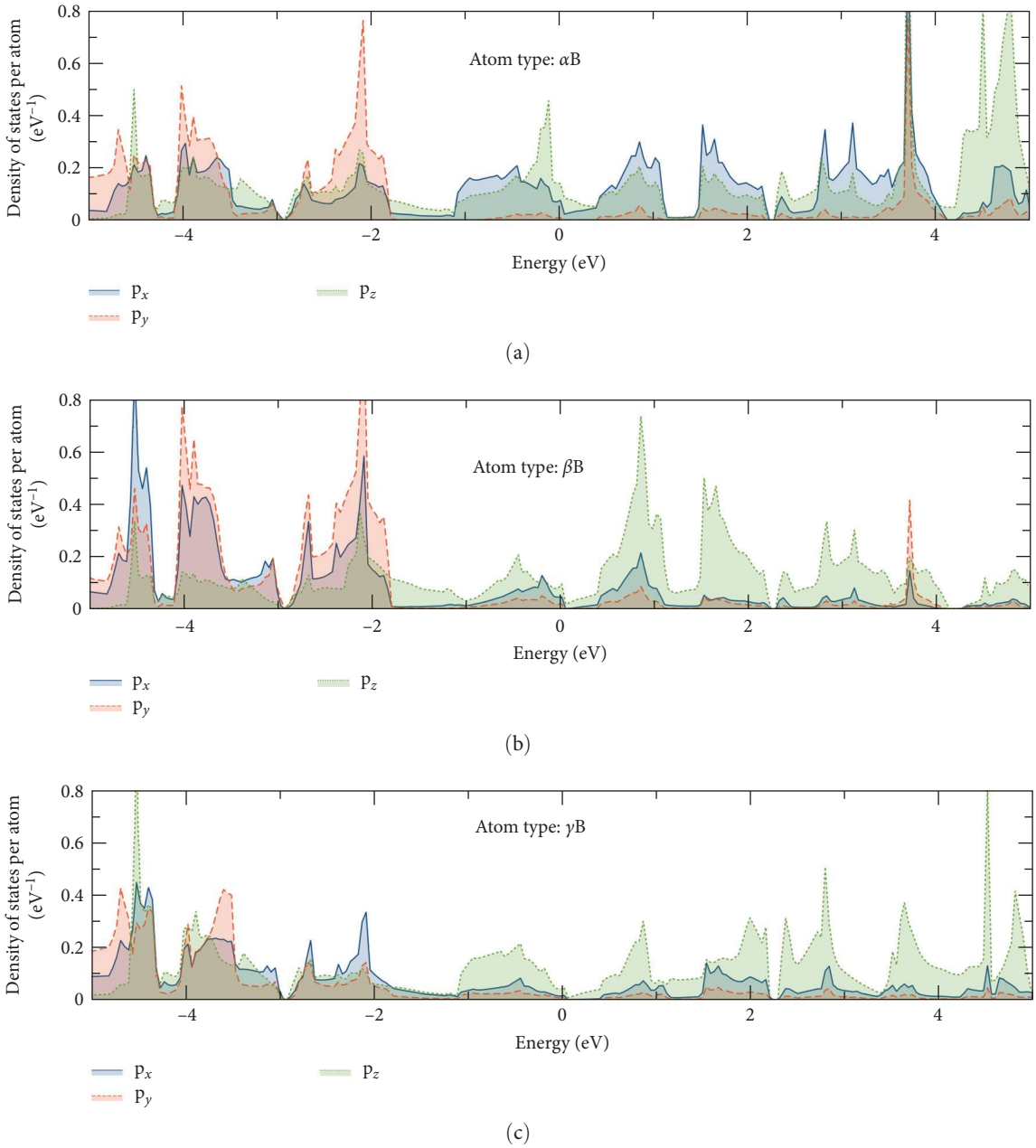

FIGURE 5: PDOS projected on p-orbitals for the (a) α, (b) β, and (c) γ types of boron atoms. The Fermi level is located at 0 eV.

the above-mentioned electrons, which are near the Fermi level and have a dominant role in conduction, have p_z orbital behavior. Also from the figure, it is possible to understand the origin of Dirac cone formations observed in the band structure near the Fermi level in between $\Gamma - X$ region and $Y - \Gamma$ region. Dirac cone formation between $\Gamma - X$ region is mostly dominated by p_z orbital of α type of boron, however Dirac cone formation between $Y - \Gamma$ region is dominated by p_z orbital of all boron types and p_x orbital of α type of boron. Therefore, it can be argued that the α type of boron has an important role in explaining the Dirac formations, which are important because of having unique electronic properties, near the Fermi level. It may be possible to argue that α type of boron atoms is also important because the structural anisotropy of the Ogee-Borophene is caused by them. By removing the α type of boron atoms from the structure, the hollows of the system will become isotropic.

In Figure 6, isosurfaces of electron density distributions with blue and yellow isosurfaces are shown for densities of 0.1 and 0.15 $a_0^{-3/2}$, respectively. Anisotropy in a bond between two boron atoms can be observed in yellow isosurfaces. Furthermore, it can be suggested that the variations in the bond lengths within the structure, gave a potential for different interaction strengths along the decagon-shaped hollows compared to the bridges between the gaps.

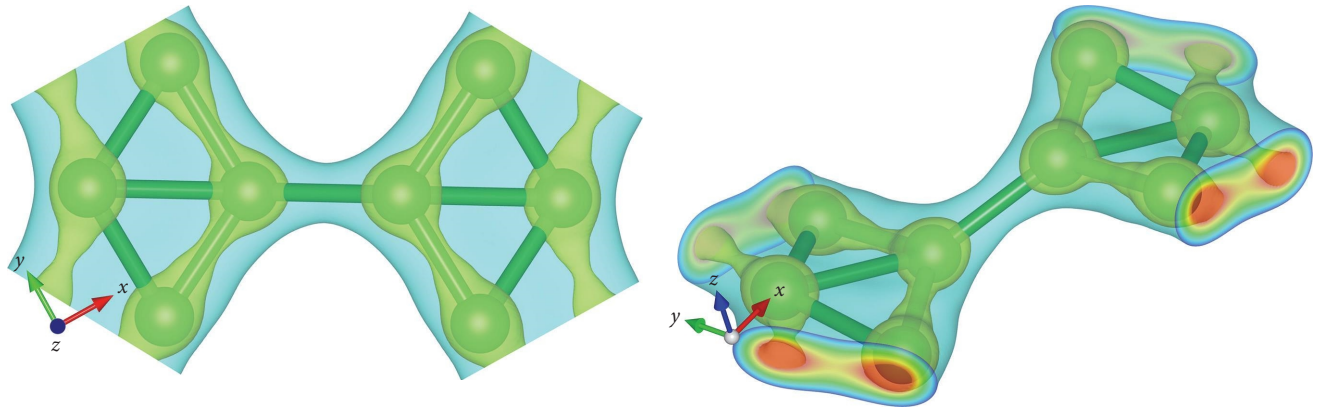

Figure 6: Electron density distributions from (a) top-view and (b) perspective view of the unit cell. Blue and yellow isosurfaces correspond to 0.1 and 0.15 $a_0^{-3/2}$, respectively. Sections at the unit-cell boundaries are also shown.

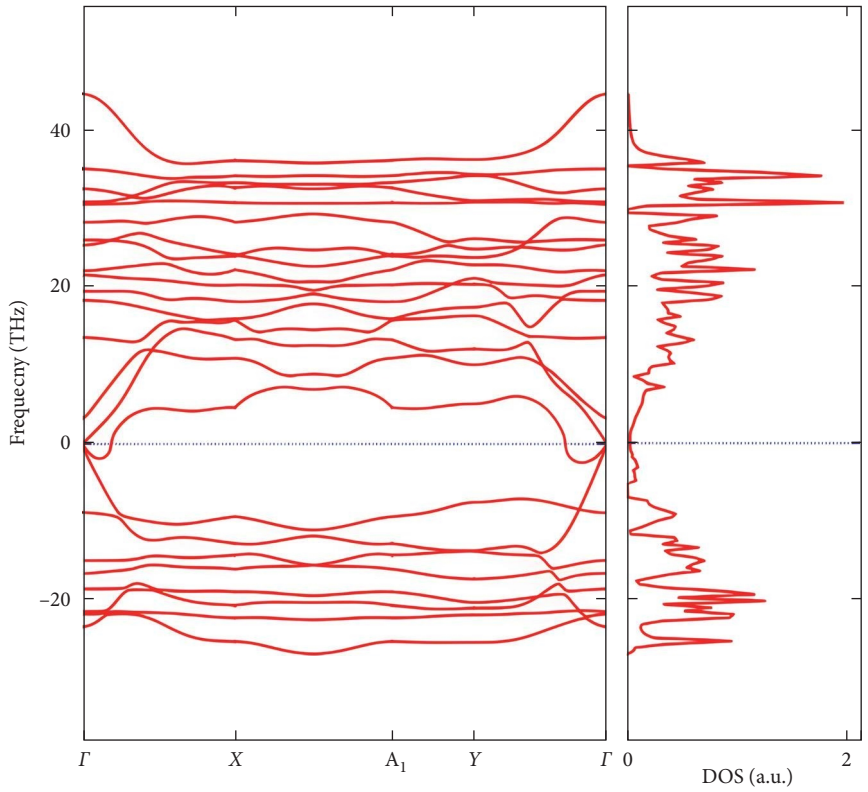

Figure 7: Phonon dispersion curves and phonon DOS for the investigated Ogee-Borophone structure (imaginary frequencies are shown as negative values).

Figure 7 shows the calculated phonon dispersion curves and the phonon DOS for the Ogee-Borophene structure. The calculated phonon dispersion curves contain many phonon branches with imaginary frequencies across the entire k-space. Imaginary frequencies are mostly regarded as the inherent structural instability of the investigated structure. However, the presence of imaginary frequencies in the phonon spectrum can provide valuable insight into the nature and properties of a material [43]. The investigation of Ogee-Borophene in this study suggests that the "free-standing" form of this polymorph is not thermodynamically stable. The term "free-standing" refers to the isolated Ogee-Borophene structure without any substrate or support. Decagonal-shaped hollows and anisotropy of the structure may contribute to its potential instability in free-standing form. However, it is worth considering the possibility of achieving stability by investigating the Ogee-Borophene on known metallic or semiconductor surfaces, which we may call a substrate. By introducing a substrate, that can provide structural support and influence the interaction between

Ogee-Borophene and its surroundings, it may be possible to stabilize the structure. Further DFT calculations and molecular dynamics simulations can help elucidate the energetic, adhesion, and electronic coupling between Ogee-Borophene and the possible substrates. These studies can guide the selection of optimal substrate materials and conditions for stabilizing Ogee-Borophene.

4. Conclusion

This study presents first-principle DFT calculations of a new hollow irregular decagon-shaped vacancy-mediated polymorph of borophene, named Ogee-Borophene. The irregular shape of the hollow decagon gives rise to different electronic properties for different atoms near the hollow decagons. Based on the DFT calculations, three types of boron atoms with distinct electronic properties, denoted as α, β, and γ, are found in this hypothetical boron polymorph. The electronic band structure shows metallic behavior with a Dirac cone far above the Fermi level. DOS and PDOS of the investigated structure show that conductivity is mostly dominated by the p_z orbital of the α-type boron atom. Our study demonstrates the different electronic properties of different boron atoms provide tuning or selective interaction functionality to this hypothetical 2D metallic polymorph. The unique electronic properties of this material, arising from the anisotropy of the structure and the presence of boron atoms with different electronic properties, suggest that Ogee-Borophene has the potential to be used in a variety of applications, including transistors, selective sensor applications without the need for doping.

The study also found that Ogee-Borophene cannot be found in a free-standing stable form. However, the possibility of obtaining stability by investigating the interaction with substrates or building heterostructured 2D materials provides a promising direction for further research.

Overall, the present study makes a significant contribution to the scientific community by providing new insights and approaches into the fundamental properties of borophene and demonstrating the potential of this material for a variety of applications.

Data Availability

The data used to support the findings of this study are available from the corresponding author upon request.

Conflicts of Interest

The authors declare that they have no conflicts of interest.

Acknowledgments

The numerical calculations reported in this paper were partially performed at TUBITAK ULAKBIM, High Performance and Grid Computing Center (TRUBA resources), and the National Center for High-Performance Computing of Turkey (UHeM) under grant number 1012802022.

References

[1] A. K. Geim, "Graphene: status and prospects," *Science*, vol. 324, no. 5934, pp. 1530–1534, 2009.

[2] R. Mas-Balleste, C. Gomez-Navarro, J. Gomez-Herrero, and F. Zamora, "2D materials: to graphene and beyond," *Nanoscale*, vol. 3, no. 1, pp. 20–30, 2011.

[3] F. R. Fan, R. Wang, H. Zhang, and W. Wu, "Emerging beyond-graphene elemental 2D materials for energy and catalysis applications," *Chemical Society Reviews*, vol. 50, no. 19, pp. 10983–11031, 2021.

[4] Q. Guo, J. Liu, C. Bai, N. Chen, and L. Qu, "2D silicene nanosheets for high-performance zinc-ion hybrid capacitor application," *ACS Nano*, vol. 15, no. 10, pp. 16533–16541, 2021.

[5] F. Bechstedt, P. Gori, and O. Pulci, "Beyond graphene: clean, hydrogenated and halogenated silicene, germanene, stanene, and plumbene," *Progress in Surface Science*, vol. 96, no. 3, Article ID 100615, 2021.

[6] Y. Hu, J. Liang, Y. Xia et al., "2D arsenene and arsenic materials: fundamental properties, preparation, and applications," *Small*, vol. 18, no. 9, Article ID 2104556, 2022.

[7] T. J. Macdonald, A. J. Clancy, W. Xu et al., "Phosphorene nanoribbon-augmented optoelectronics for enhanced hole extraction," *Journal of the American Chemical Society*, vol. 143, no. 51, pp. 21549–21559, 2021.

[8] X. Wang, X. Yu, J. Song et al., "Two-dimensional semiconducting antimonene in nanophotonic applications—a review," *Chemical Engineering Journal*, vol. 406, Article ID 126876, 2021.

[9] F.-F. Zhu, W.-J. Chen, Y. Xu et al., "Epitaxial growth of two-dimensional stanene," *Nature Materials*, vol. 14, no. 10, pp. 1020–1025, 2015.

[10] F. Yang, A. O. Elnabawy, R. Schimmenti et al., "Bismuthene for highly efficient carbon dioxide electroreduction reaction," *Nature Communications*, vol. 11, no. 1, pp. 1–8, 2020.

[11] W. Wu, G. Qiu, Y. Wang, R. Wang, and P. Ye, "Tellurene: its physical properties, scalable nanomanufacturing, and device applications," *Chemical Society Reviews*, vol. 47, no. 19, pp. 7203–7212, 2018.

[12] Y. V. Kaneti, D. P. Benu, X. Xu, B. Yuliarto, Y. Yamauchi, and D. Golberg, "Borophene: two-dimensional boron monolayer: synthesis, properties, and potential applications," *Chemical Reviews*, vol. 122, no. 1, pp. 1000–1051, 2022.

[13] C. Hou, G. Tai, J. Hao, L. Sheng, B. Liu, and Z. Wu, "Ultrastable crystalline semiconducting hydrogenated borophene," *Angewandte Chemie International Edition*, vol. 59, no. 27, pp. 10819–10825, 2020.

[14] J. Hao, G. Tai, J. Zhou, R. Wang, C. Hou, and W. Guo, "Crystalline semiconductor boron quantum dots," *ACS Applied Materials & Interfaces*, vol. 12, no. 15, pp. 17669–17675, 2020.

[15] Z. Wu, G. Tai, W. Shao, R. Wang, and C. Hou, "Experimental realization of quasicubic boron sheets," *Nanoscale*, vol. 12, no. 6, pp. 3787–3794, 2020.

[16] B. Kiraly, X. Liu, L. Wang et al., "Borophene synthesis on Au (111)," *ACS Nano*, vol. 13, no. 4, pp. 3816–3822, 2019.

[17] R. Wu, I. K. Drozdov, S. Eltinge et al., "Large-area single-crystal sheets of borophene on Cu (111) surfaces," *Nature Nanotechnology*, vol. 14, no. 1, pp. 44–49, 2019.

[18] Z. A. Piazza, H.-S. Hu, W.-L. Li, Y.-F. Zhao, J. Li, and L.-S. Wang, "Planar hexagonal B36 as a potential basis for extended single-atom layer boron sheets," *Nature Communications*, vol. 5, Article ID 3113, 2014.

[19] A. P. Sergeeva, I. A. Popov, Z. A. Piazza et al., "Understanding boron through size-selected clusters: structure, chemical bonding, and fluxionality," *Accounts of chemical research*, vol. 47, no. 4, pp. 1349–1358, 2014.

[20] I. Boustani, "Systematic ab initio investigation of bare boron clusters: determination of the geometry and electronic structures of B_n (n = 2−14)," *Physical Review B*, vol. 55, no. 24, pp. 16426–16438, 1997.

[21] Y. Huang, S. N. Shirodkar, and B. I. Yakobson, "Two-dimensional boron polymorphs for visible range plasmonics: a first-principles exploration," *Journal of the American Chemical Society*, vol. 139, no. 47, pp. 17181–17185, 2017.

[22] Y. Xu, X. Xuan, T. Yang, Z. Zhang, S.-D. Li, and W. Guo, "Quasi-freestanding bilayer Borophene on Ag (111)," *Nano Letters*, vol. 22, no. 8, pp. 3488–3494, 2022.

[23] X. Liu, Q. Li, Q. Ruan, M. S. Rahn, B. I. Yakobson, and M. C. Hersam, "Borophene synthesis beyond the single-atomic-layer limit," *Nature Materials*, vol. 21, no. 1, pp. 35–40, 2022.

[24] Y. Yu, K. Zhang, H. Parks et al., "Tunable angle-dependent electrochemistry at twisted bilayer graphene with moiré flat bands," *Nature Chemistry*, vol. 14, no. 3, pp. 267–273, 2022.

[25] J. Wang, Y. Liu, and Y.-C. Li, "A new class of boron nanotube," *ChemPhysChem*, vol. 10, no. 17, pp. 3119–3121, 2009.

[26] A. J. Mannix, X.-F. Zhou, B. Kiraly et al., "Synthesis of borophenes: anisotropic, two-dimensional boron polymorphs," *Science*, vol. 350, no. 6267, pp. 1513–1516, 2015.

[27] A. J. Mannix, Z. Zhang, N. P. Guisinger, B. I. Yakobson, and M. C. Hersam, "Borophene as a prototype for synthetic 2D materials development," *Nature Nanotechnology*, vol. 13, no. 6, pp. 444–450, 2018.

[28] M. Ou, X. Wang, L. Yu et al., "The emergence and evolution of borophene," *Advanced Science*, vol. 8, no. 12, Article ID 2001801, 2021.

[29] E. S. Penev, S. Bhowmick, A. Sadrzadeh, and B. I. Yakobson, "Polymorphism of two-dimensional boron," *Nano Letters*, vol. 12, no. 5, pp. 2441–2445, 2012.

[30] H. Tang and S. Ismail-Beigi, "Novel precursors for boron nanotubes: the competition of two-center and three-center bonding in boron sheets," *Physical Review Letters*, vol. 99, no. 11, Article ID 115501, 2007.

[31] Y. Zhao, S. Zeng, and J. Ni, "Phonon-mediated superconductivity in borophenes," *Applied Physics Letters*, vol. 108, no. 24, Article ID 242601, 2016.

[32] Z. Zhang, Y. Yang, G. Gao, and B. I. Yakobson, "Two-dimensional boron monolayers mediated by metal substrates," *Angewandte Chemie*, vol. 127, no. 44, pp. 13214–13218, 2015.

[33] Y. Liu, E. S. Penev, and B. I. Yakobson, "Probing the synthesis of two-dimensional boron by first-principles computations," *Angewandte Chemie International Edition*, vol. 52, no. 11, pp. 3156–3159, 2013.

[34] X. Wu, J. Dai, Y. Zhao, Z. Zhuo, J. Yang, and X. C. Zeng, "Two-dimensional boron monolayer sheets," *ACS Nano*, vol. 6, no. 8, pp. 7443–7453, 2012.

[35] G. Bhattacharyya, A. Mahata, I. Choudhuri, and B. Pathak, "Semiconducting phase in borophene: role of defect and strain," *Journal of Physics D: Applied Physics*, vol. 50, no. 40, Article ID 405103, 2017.

[36] B. Feng, J. Zhang, Q. Zhong et al., "Experimental realization of two-dimensional boron sheets," *Nature Chemistry*, vol. 8, no. 6, pp. 563–568, 2016.

[37] A. H. Larsen, J. J. Mortensen, J. Blomqvist et al., "The atomic simulation environment—a Python library for working with atoms," *Journal of Physics: Condensed Matter*, vol. 29, no. 27, Article ID 273002, 2017.

[38] J. Enkovaara, C. Rostgaard, J. J. Mortensen et al., "Electronic structure calculations with GPAW: a real-space implementation of the projector augmented-wave method," *Journal of Physics: Condensed Matter*, vol. 22, no. 25, Article ID 253202, 2010.

[39] J. J. Mortensen, L. B. Hansen, and K. W. Jacobsen, "Real-space grid implementation of the projector augmented wave method," *Physical Review B*, vol. 71, no. 3, Article ID 035109, 2005.

[40] S. B. Lisesivdin and B. Sarikavak-Lisesivdin, "*gpaw-tools*—higher-level user interaction scripts for GPAW calculations and interatomic potential based structure optimization," *Computational Materials Science*, vol. 204, Article ID 111201, 2022.

[41] K. Momma and F. Izumi, "VESTA 3 for three-dimensional visualization of crystal, volumetric and morphology data," *Journal of Applied Crystallography*, vol. 44, no. 6, pp. 1272–1276, 2011.

[42] A. Togo, "First-principles Phonon calculations with Phonopy and Phono3py," *Journal of the Physical Society of Japan*, vol. 92, no. 1, Article ID 012001, 2023.

[43] I. Pallikara, P. Kayastha, J. M. Skelton, and L. D. Whalley, "The physical significance of imaginary phonon modes in crystals," *Electronic Structure*, vol. 4, no. 3, Article ID 033002, 2022.